

T H E U N I V E R S I T Y O F M I C H I G A N

COLLEGE OF ENGINEERING
Department of Aerospace Engineering

First Annual Report

MODEL OF AN ELECTRIC ARC BALANCED MAGNETICALLY IN A GAS FLOW

Arnold M. Kuethe
Robert L. Harvey
Leland M. Nicolai

ORA Project 07912

supported by:

NATIONAL AERONAUTICS AND SPACE ADMINISTRATION
GRANT NO. NGR-23-005-128
WASHINGTON, D. C.

administered through:

OFFICE OF RESEARCH ADMINISTRATION ANN ARBOR

April 1967

TABLE OF CONTENTS

	Page
LIST OF FIGURES	v
1. INTRODUCTION	1
2. ARC AS A STEADY PHENOMENON	2
3. THE ARC AS AN IMPERVIOUS BODY	3
4. GENERAL EQUATIONS	4
5. GENERAL PROPERTIES OF INTERNAL FLOW	6
6. CIRCULATION WITHIN THE CORE	10
7. THE BOUNDARY LAYER	13
8. MEASURED PROPERTIES	15
9. CONCLUSIONS	16
10. REFERENCES	17

LIST OF FIGURES

Figure	Page
1. Relative orientation of the velocity, magnetic, and electric fields.	18
2. Polaroid photograph of arc reflection in side-wall of tunnel. $M_\infty = 2.5$, $P_t = 12.9$ in. Hg, $I = 425$ amp, gap = 1.1 in.	19
3. Film sequence showing particle moving from anode (bottom) to cathode. $M_\infty = 2.5$, film speed about 3000 exposures per second.	19
4. Film sequence showing two views of particle moving from anode (bottom) to cathode in the column wake. $M_\infty = 2.5$, film speed about 4700 exposures per second.	20
5. Qualitative model of balanced arc.	21
6. Heat transfer from arc relative to that from solid cylinder versus Lorentz convection parameter.	22
7. Boundary layer formation.	22
8. Current density and arc dimensions for $M_\infty = 2.5$.	23
9. Current density and arc dimensions for $M_\infty = 3.5$.	24
10. Normal force coefficient referred to the normal velocity component versus the normal Reynolds number based upon free stream properties.	25

1. INTRODUCTION

A persistent problem relative to a convected or balanced arc has been that of determining whether the arc simulates a solid cylinder or whether the phenomenon is a "flow-through" process. In this report a fluid mechanical model of the steady arc is developed on the basis of photographs which show that the arc must simulate a solid body.*

The experimental data were obtained on the equipment developed by Bond,¹ and on which he showed for the first time that an arc could be balanced magnetically in a high-speed airstream and that the arc is stable in a supersonic flow if it can assume a characteristic slant angle near the Mach angle of the incident flow. Other significant properties of the balanced arc are also given in these references. Figure 1 demonstrates the relative orientation of the velocity, magnetic, and electric fields for the balanced arc. The intensity of the external magnetic field was around 20 times that of the self-field.

In the following sections evidence is given that, with some qualifications (1) the balanced arc can be treated as a steady phenomenon, (2) the dynamics of the arc plasma in a uniform magnetic field can be treated by the equations of continuum fluid mechanics, (3) the arc simulates approximately an infinite solid cylinder of uniform cross section, and (4) the internal flow and a boundary layer flow can be treated separately. The dimensionless parameters, the governing equations and the boundary conditions are discussed and the equations simplified for the inner and outer flows.

The authors gratefully acknowledge helpful discussions with Professors R. L. Phillips and S. W. Bowen on various aspects of arc technology and diagnostic techniques.

*This report is an expanded version of the preprint AIAA paper No. 67-96 with the same title.

2. ARC AS A STEADY PHENOMENON

High-speed motion pictures by Bond¹ showed for the first time that an arc can be balanced magnetically as well as stabilized in a cross flow. The arc was balanced magnetically between rails in a supersonic flow; the configuration of electric, magnetic, and flow fields are shown in Fig. 1. High-speed motion pictures showed that a remarkably steady, sharply defined, arc column could be achieved if the magnetic field intensity decreased with distance upstream, and the streamwise location of the balance between the aerodynamic and Lorentz forces determined anode and cathode root locations on the rail electrodes such that the arc could assume a characteristic slant angle as shown in the photograph of Fig. 2. The slant, measured from the stream direction was found to be a few degrees greater than the Mach angle and independent of all other properties of the flow or of the arc. Bond showed further that the ionization parameter E/P_t (the ratio of the voltage drop along the arc to the pressure at the stagnation point for the cross-flow past an inclined cylinder) is a maximum when the slant angle is equal to the Mach angle; thus the steady balanced arc in a supersonic flow tends to align itself so that the degree of ionization is a maximum.

3. THE ARC AS AN IMPERVIOUS BODY

An axial flow along the arc, which is a sufficient condition that the exterior stream flows around rather than through the arc, was observed by the first two authors.² High-speed motion pictures taken in the setup described in Ref. 1 show small masses of vaporizing copper moving along the arc from anode to cathode; two such sequences are shown in Figs. 3 and 4.

The vaporizing particle shown in the nearly head-on sequence of Fig. 3 moves along the arc at about 35 ft/sec, while the speed of the free stream is about 1800 ft/sec. The proof that the arc simulates a solid cylinder lies in the fact that if the flow were through the arc, rather than around it, the vaporizing particle would be swept downstream long before it could reach the cathode.

The sequence reproduced in Fig. 4 shows two simultaneous views of the arc, one nearly head-on, the other the reflected image in a chromium mirror forming the side-wall of the tunnel. A vaporizing particle of magnesium is shown in the two views in frame 2 of Fig. 4 is just behind the arc. The successive frames show the motion along a path inclined upward and downstream, indicating that the air speed in the wake is extremely low. An interesting feature in frame 2 is that the vaporizing particle is photographed through the arc indicating that the arc is not opaque to at least some of the magnesium radiation.

The measured speeds of particles along the arc give a lower bound of the axial flow speed because of the weight of the vaporizing particles being photographed; the cathode is above the anode so the gravitational force retards the upward motion of the particles. In one run a particle actually remained stationary within the arc for several frames indicating that its weight was equal to the drag exerted on it by the axial flow. Experiments utilizing injected gases instead of solid particles are under preparation.

The tracer studies were made in the slanted arc at Mach 2.5 and 3.5. Roman³ has since, on the basis of photographs and flow measurements confirmed the solid cylinder simulation for a balanced arc in a subsonic free jet.

4. GENERAL EQUATIONS

We assume here that the arc column approximates a cylinder of constant cross-section so that the flow, both internal and external, may be treated as two dimensional relative to coordinates in the plane normal to the axis of the arc. The approximation will be far from reality near the roots but experimental results indicate satisfactory agreement at stations midway between the arc roots, particularly if the ratio of the arc length to the major lateral dimension is large. The cylinder is impervious to the external flow but mass transfer from the arc to the external stream takes place; the mass transferred is assumed to be supplied by the axial flow indicated by Figs. 3 and 4.

Estimates (see Section 5) indicate that the average arc temperatures at Mach 2.5 over the range of operating conditions in air are around 8000°K. We may therefore treat the arc plasma as weakly ionized. Also, radiation and nonequilibrium effects are neglected and we approximate the conservation equations for the flow field within the arc by those for a perfect gas:

$$\rho(\vec{V} \cdot \nabla)\vec{V} = -\nabla P + \vec{J} \times \vec{B} + \nabla(\mu \nabla \cdot \vec{V}) \quad (1)$$

$$P + c_p \vec{V} \cdot \nabla T = \vec{V} \cdot \nabla P + \nabla(k \nabla T) + \frac{J^2}{\sigma} + \Phi \quad (2)$$

$$\nabla \cdot (\rho \vec{V}) = \epsilon(x, y) \quad (3)$$

ρ , \vec{V} , P , μ , k , T , Φ are, respectively, the fluid density, velocity, pressure, viscosity, heat conduction, temperature, and rate of viscous dissipation; \vec{J} is the current density, \vec{B} the magnetic induction, \vec{E} the electric field, ϵ the source strength (mass drawn per second from the axial flow to make up for the rate of transfer to the free stream at the boundary).

Since the external magnetic field is around 20 times that of the self-field the magnetic induction \vec{B} is taken as constant and equal to that for the external field. The plasma velocity will be small and if we neglect Hall currents,

$$\left. \begin{aligned} \vec{J} &= \sigma \vec{E} = \vec{J}(T) \\ \frac{J^2}{\sigma} &= \vec{E} \cdot \vec{J} \end{aligned} \right\} \quad (4)$$

In the experimental setup used, the airflow is in the x direction, $\vec{B} = B\vec{e}_y$, where \vec{e}_y is the unit vector in the y direction, and $\vec{J} = J\vec{e}_z$. Then

$$\vec{J} \times \vec{B} = -JB\vec{e}_x \quad (5)$$

In succeeding sections these equations will be specialized for the internal and external flows.

5. GENERAL PROPERTIES OF INTERNAL FLOW

Equations (1) through (5) describe a circulation generated by a variable Lorentz force $-J\vec{B}_x$ acting upstream on an element of plasma within the balanced arc; the phenomenon is conceptually analogous to the generation of convection currents by gravity forces acting on a nonuniformly heated gas contained within a horizontal cylindrical tube heated over the central region. The electric current density within the arc is in general a maximum at the center; then an element with current density greater than that required by the balance between Lorentz and pressure force will be accelerated toward the upstream boundary. Schematic streamlines are shown in Fig. 5, which shows flow separation at the vertices of the elliptical cross-section. This feature was shown specifically by Roman's measurements³; the photographs in Fig. 4 also indicate that wake velocities are low. We show in Section 6 that EJ, the joule heating term in Eq. (2), is much larger than the diffusion term in the interior of the arc so that the temperature of the element and, therefore, the electric current density will increase while the element moves toward the upstream boundary while the pressure gradient generated in the external flow deflects the element in the streamwise direction along the boundary. At some point near the boundary the diffusion term in Eq. (2) will dominate and the elements in the vicinity will suffer a decrease in temperature, current density, and Lorentz force. Some of the arc plasma will accordingly be sufficiently cooled by diffusion and sufficiently accelerated by the pressure gradient along the boundary to be swept downstream in the wake. However, a portion of the plasma will presumably retain sufficient current density to remain within the arc and be reheated as it circulates in what resembles a double eddy pattern. Calculations by Fischer and Uhlenbusch⁴ indicate that the "double-eddy" circulation also occurs in a wall stabilized arc in an external orthogonal magnetic field.

The balanced arc becomes steady where an equilibrium current density or temperature distribution is reached such that; the temperature gradients at the boundary are just great enough to transfer to the external flow the heat that is carried to the boundary, mainly by the internal circulation. The intensity of this circulation will be determined by the degree of non-uniformity of the current density within a core. The process has a stabilizing feature in that, if the circulation is not sufficient to carry to the boundary all of the heat generated, the nonuniformity of the temperature and current density distributions will be accentuated with a resulting intensification of the circulation to carry the excess heat to the boundary.

The streamlines shown in Fig. 5 are schematically the projections of the paths of fluid elements on the arc cross-section. The rate of mass transfer to the external flow at a given station along the arc is, under steady condi-

tions, equal to the source strength at that station (see Eq. (3)). It is clear that the rate of mass transferred at the boundary must be small compared with the rate of axial mass flow, in order that departures from effective two dimensionality of the internal flow may be neglected.

As a result of the internal circulation, the plasma properties will tend toward uniformity over the cross-section. It follows that the more intense the circulation the greater will be the tendency toward uniformity over a core and, hence, toward the formation of a "boundary layer" at the arc boundary within which large gradients in momentum, temperature, and density exist. For steady conditions the circulation must be just intense enough to transfer the energy generated, EI per second, to the boundary of the core.

The arc boundary will be the locus of the balance between magnetic and fluid pressures, that is, if the speeds associated with internal circulation are low enough so that local pressures are not affected, the equation

$$p_u = p_d + \int_{x_d}^{x_u} JBdx \quad (6)$$

(subscripts u and d designate upstream and downstream values) expresses the equilibrium condition at every point of the boundary. The boundary shape thus determined will depend on the incident velocity, gas density and pressure, on the electric current and current density, on the external and self magnetic fields, on flow interference caused by other bodies in the vicinity, stream boundaries, etc.

The above flow can be expressed in terms of the conservation equations in forms analogous to those used to describe heat convection. The following nondimensional parameters are defined:

$$\left. \begin{aligned} j &= \frac{J}{J_1}, \quad \vec{u} = \frac{\vec{V}}{U_1}, \quad p = \frac{P}{\bar{\rho}U_1^2}, \quad x = \frac{X}{d}, \quad y = \frac{Y}{d} \\ \pi &= \frac{U_1 t}{d}, \quad \theta = \frac{T}{T_1}, \quad Re_1 = \frac{\bar{\rho}U_1 d}{\bar{\mu}}, \quad L_c = \frac{\bar{\rho}J_1 B d^3}{\bar{\mu}^2} \\ Pr_1 &= \frac{c_p \bar{\mu}}{k}, \quad K_1 = \frac{U_1^2}{c_p T_1}, \quad S = \frac{E J_1 d}{\bar{\rho} c_p T_1 U_1} \end{aligned} \right\} (7)$$

For the purpose of comparing orders of magnitude of the various terms ρ and μ are replaced by their average values, $\bar{\rho}$ and $\bar{\mu}$. Then Eqs. (1) through (3), with relations (4) and (5), are nondimensionalized, and, with the parameters

defined in Eq. (7), they become

$$\frac{d\vec{u}}{d\tau} = \text{grad } p - \frac{L_c}{\text{Re}_1^2} j \vec{e}_x + \frac{1}{\text{Re}_1} \nabla^2 \vec{u} \quad (8)$$

$$\frac{d\theta}{d\tau} = K_1 \frac{dp}{d\tau} - \frac{1}{\text{Pr}_1 \text{Re}_1} \nabla^2 \theta + Sj + \frac{K_1}{\text{Re}_1} \phi \quad (9)$$

$$\text{div } \vec{u} = \frac{\epsilon d}{U_1 \bar{\rho}} \quad (10)$$

where d is a characteristic length and U_1 , T_1 , and J_1 are, respectively, characteristic velocity, temperature, and current density.

In addition to the Reynolds (Re_1), Prandtl (Pr_1), and Eckert (K_1) numbers, the following parameters are significant in determining the physical aspects of the internal flow.

The role of L_c , termed here the Lorentz convection parameter, in determining the intensity of the circulation within the arc is roughly analogous to that of the Grashof number, $\beta g \Delta \theta d^3 / \nu^2$ (β is the expansion coefficient of the fluid, g is the acceleration of gravity, and $\Delta \theta = \Delta T / T_1$) in determining the intensity of the circulation of a gas generated by gravitational convection within a horizontal cylinder with nonuniform temperature distribution over the cross-section. We see that in the Lorentz convection parameter the Lorentz acceleration $jB/\bar{\rho}$ replaces the gravitational acceleration $\beta g \Delta \theta$ in the Grashof number. Reference to Eq. (8) shows that the ratio of the Lorentz to the viscous force on a representative element is L_c / Re_1 , and the Lorentz to the inertia force is L_c / Re_1^2 . In the analysis given here we write $J_1 d^2 = I$, so that

$$L_c = \frac{\bar{\rho} I B d}{\mu^2} \quad (11)$$

A qualitative analogy between the circulation within a balanced arc and that in a horizontal internally heated cylinder of gas is to be expected, even though the joule heating term EJ (or Sj in Eq. (9)) has no counterpart in the convection problem. In fact, the effect of this term is to intensify the internal circulation, since an element is being heated continuously during its motion. It therefore experiences a continuous increase in current density and thus in Lorentz force (provided, as is indicated in Section 6 the heat generation rate is greater than the heat transfer rate from the element).

The characteristic velocity for the internal flow is not known; we show in the next section on the basis of experimental results that a characteristic velocity

$$V_1 = \sqrt{\frac{J_1 B}{\bar{\rho}}} d_f \quad (12)$$

where d_f is the cross-stream dimension of the arc is nearly constant over a wide range of conditions at Mach 2.5. It thus exhibits the desired property of a characteristic velocity. Further,

$$Re_1 = \sqrt{L_c} \quad (13)$$

so that Eq. (8) may be written

$$\frac{d\vec{u}}{dt} = -\text{grad } p - j \vec{e}_x + \frac{1}{\sqrt{L_c}} \nabla^2 \vec{u} \quad (14)$$

For high values of the Lorentz parameter Eq. (14) is of the boundary layer type, since the coefficient of the highest order term is small. The balanced arc will therefore consist of an inner core of relatively uniform properties and a thin boundary layer within which the properties change through high gradients from their core values to those in the free stream. Equation (14) indicates that the higher the Lorentz parameter the thinner will be the boundary layer. We may reason further that, since over the arc temperature range indicated by the gross properties (6000° to 8000°K) the Prandtl number is near unity, the temperature boundary layer will also be thin.

More important than the Prandtl number however is the effect of joule heating, the term Sj in Eq. (9). If the pressure gradient term is eliminated between Eqs. (8) and (9), viscous dissipation is neglected, and the velocities are assumed low enough so that their squares can be neglected relative to the enthalpy level within the arc, we obtain

$$\frac{d\theta}{d\tau} = \frac{1}{Pr Re_1} \nabla^2 \theta + j(S - u_1 K) \quad (14a)$$

where u_1 is the x component of the velocity. Within the arc $S \gg u_1 K$ and $jS \gg (Pr Re_1)^{-1} \nabla^2 \theta$ so that an element will be heated continuously as it is connected toward the boundary. As it is heated the current density and therefore the Lorentz force increase and it must encounter a very high $\nabla^2 \theta$ before the rate of heat diffusion from the element will be greater than that added by joule heating; this high $\nabla^2 \theta$ will mark the boundary of the arc core and the inner edge of the boundary layer.

6. CIRCULATION WITHIN THE CORE

Equations (1) through (3) applied to the core flow may be simplified if we may consider the flow field as generated by a perturbation on a uniform current density J_0 . This superposition is justified if the velocities generated are small and if the flow is incompressible. Then we may write

$$J = J_0 + J'(x,y) \quad (15)$$

where $J_0 = \text{constant}$ and $-J_0 B e_x^{\rightarrow}$ is equal to the average pressure gradient required to balance the arc, that is,

$$\frac{\partial p}{\partial x} = -J_0 B e_x^{\rightarrow} \quad (16)$$

This equation agrees with Eq. (6) for constant current density. Then Eq. (8), which already postulates incompressible flow, becomes

$$\frac{d\vec{u}}{dt} = -\frac{L_c}{Re_1^2} J' e_x^{\rightarrow} - \frac{\partial p}{\partial y} e_y^{\rightarrow} + \frac{1}{Re} \nabla^2 \vec{u} \quad (17)$$

where $j = J'/J_0$ and $J_0 = J_1$ in Eq. (10).

Comparison of the rate of heat transfer from the balanced arc with that calculated for a solid cylinder at the same temperature indicates a trend consistent with the boundary layer hypothesis. Figure 6 is a plot of EI/Q versus L_c for observations at Mach 2.5 and 3.5; Q is the calculated rate of heat transfer from a solid cylinder 5, 6, 7 at the same temperature and with cross-sectional area equal to that of the arc as indicated by two simultaneous photographs such as those shown in Fig. 4, EI is the rate of joule heating within the arc. In Eq. (11) for L_c , $\bar{\rho}$ and $\bar{\mu}$ are taken as the mean values over the arc, and $d = d_f$, the arc dimension normal to the flow direction. The mean temperature of the arc was approximated from the indicated cross-sectional area and the measured total current and voltage drop along the arc. The mean temperatures so calculated were between 6000° and 8000°K . Figure 6 shows that at each Mach number EI/Q increases with L_c ; this trend is consistent with the hypothesis that, under steady conditions, as the Lorentz parameter increases there is a corresponding increase in the rate of energy transfer by the internal circulation to the arc boundary, and, in turn, an increase in the temperature gradient in the boundary layer to effect the transfer of the energy to the external flow.

The quantitative values of EI/Q are remarkably close to unity considering the approximate nature of the comparison with the solid cylinder. Since we have no theory for the properties of the boundary layer between the arc plasma and the external flow there is no reason to suppose that the heat transfer from the arc will be the same function of Reynolds number and boundary temperature as for a solid cylinder. This circumstance, in addition to the fact that the values of Q were calculated by Jakob's empirical formula,⁵ based on measurements on circular cylinders at relatively low temperature.

The expression analogous to Eq. (15) is

$$T = T_0 + T'(x,y) \quad (18)$$

with $T_0 = \text{constant}$ is the temperature corresponding to current density J_0 . Then the energy equation, Eq. (9), becomes with $\theta = T'/T_0 = T'/T_1$

$$\frac{d\theta'}{d\tau} = K_1 \frac{dp}{d\tau} - \frac{1}{Pr_1 Re_1} v^2 \theta' + S(1 + j') + \frac{K_1}{Re_1} \phi \quad (19)$$

We postulate that $j' \ll 1$, $T' \ll T_0$, and, as a consequence velocities are low enough so that the first and last terms on the right are negligible. Also the diffusion term, the second on the right will be negligible compared with the joule heating term, which reduces to S . Then Eq. (19) becomes

$$\frac{d\theta'}{d\tau} = S = \text{const} \quad (20)$$

The characteristic velocity given in Eq. (12) has been calculated for all of the Mach 2.5 results with $d = d_f$, the arc width normal to the stream, and was found to have the value 4×10^3 ft/sec $\pm 25\%$ for $1.6 \times 10^4 < E_j < 10^5$, $9 < P_t < 29$ in. Hg, and $150 < I < 750$ amps. Thus,

$$V_1 = \sqrt{\frac{J_1 B}{\bar{\rho}}} d_f \quad (21)$$

is a particularly appropriate characteristic velocity for the analyses of the core flow. Equation (17) then becomes

$$\frac{d\vec{u}}{dt} = -J' \vec{e}_x - \frac{\partial p}{\partial y} \vec{e}_y + \frac{1}{\sqrt{L_c}} v^2 \vec{u} \quad (22)$$

Fischer and Uhlenbusch⁴ neglect the inertia term but the justification is not clear. We plan to investigate various forms of this equation, along

with Eq. (20) for practical values of L_c to determine the validity of the approximations.

In the continuity equation

$$\frac{\partial u}{\partial x} + \frac{\partial v}{\partial y} = \frac{\epsilon}{\rho} \quad (23)$$

it will also be necessary to determine the conditions under which ϵ can be neglected.

7. THE BOUNDARY LAYER

Figure 7 illustrates the physical process by which a momentum boundary layer is established. The pressure gradient in the flow along the surface is opposed by a component of the Lorentz force acting on an element of the plasma at the arc boundary. Thus a momentum gradient develops throughout the layer within which the current density decreases from the value representative of the arc core to substantially zero. The following example indicates that the reduction in momentum at the boundary will be considerable: At Mach 3.5, a stagnation pressure of one atmosphere, an arc current of 200 amperes, and a magnetic field of 1540 gauss, the dimensions of the luminous portion of the arc are 0.032 x 0.023 ft; assuming that the electric current density within the luminous portion of the arc is constant, $J = 5.2 \times 10^5$ amps/ft², and the Lorentz force is 5.5×10^3 lb/ft³. We now compare this force with the maximum pressure gradient in the plane normal to the slanted arc (Mach number for the velocity component normal to arc is approximately unity) for a circular cylinder of the same area as the arc.⁸ This maximum gradient is 6.1×10^3 lb/ft³; it occurs at 65° from the stagnation point. The component of the Lorentz force opposing this pressure gradient is about $0.9 \times 5.5 \times 10^3 = 5.0 \times 10^3$ lb/ft³. A close comparison of the above numbers is not meaningful but the fact that they are not significantly different indicates that an element of arc plasma at the boundary will be nearly in equilibrium and therefore that the momentum of the plasma at the arc boundary is small compared with that of the free stream.

The ratio between the density in the core and that in the free stream is about 0.01. Thus a small net force on the plasma element would cause high accelerations near the arc boundary. For this reason instead of a velocity boundary layer we must direct our consideration to the momentum layer.

Considering that virtually the entire changes in the properties take place within the boundary layer, simplifications of the conservation equations applicable throughout the layer do not appear feasible. With the ordinary boundary layer approximations Eqs. (1) and (2) become

$$\begin{aligned}
 \rho \frac{du_s}{dt} &= - \frac{\partial p}{\partial s} - JB \sin(n,x) + \frac{\partial}{\partial n} \left(\mu \frac{\partial u_s}{\partial n} \right) \\
 \rho c_p \frac{dT}{dt} &= u \frac{\partial p}{\partial x} + \frac{\partial}{\partial n} \left(k \frac{\partial T}{\partial n} \right) + EJ + \mu \left(\frac{\partial u_s}{\partial n} \right)^2 \\
 \frac{\partial}{\partial s} (\rho u_s) + \frac{\partial}{\partial n} (\rho v_s) &= 0 \\
 J &= J(T,p)
 \end{aligned}
 \tag{24}$$

with boundary conditions:

$$\text{at } n = 0: u_s = u_b, v_s = v_0, T = T_b$$

$$\text{at } n = \infty: u_s = u_\infty, T = T_\infty$$

where u_b and T_b are properties at the boundary of the core.

The boundary conditions at $n = 0$, as well as the shape of the boundary corresponding to $n = 0$, must be given by the solutions in the core described by the equations given in Section 6.

8. MEASURED PROPERTIES

Measurements of the arc dimensions were made relatively easy by the fact that the arc boundary at least over the upstream portion is quite distinct, as is shown in Figs, 2, 3, and 4. This circumstance supports the indication given here that a thin boundary layer exists through which the transfer takes place.

Figures 8 and 9 show some arc dimensions at Mach 2.5 and 3.5, at atmospheric stagnation pressure. The dimensions were measured by means of simultaneous photographs of a head-on view and a view of the arc reflected at the tunnel wall. The ratio of d_f , the arc dimension normal to the stream to d_s that parallel to the streams, is about 1.3 over the range of arc currents from 130 to 500 amperes.

The calculated values of current density are based on the assumptions that the luminous portion represents the core of relatively constant properties and that the cross-section as elliptical; the calculated temperatures are being checked by diffraction measurements. The voltage drop along the column, measured at two electrode gaps, varied from 20 to 30 volts per inch. The values of the normal force coefficient versus Reynolds number for the component normal to the arc are shown for two Mach numbers in Fig. 10. The values show considerable variation with Mach number but the values are in the range of measured drag coefficients for solid circular cylinders at Mach numbers around one.⁹

9. CONCLUSIONS

On the basis of high-speed motion pictures of tracers we conclude that a magnetically balanced steady arc in a cross flow is impervious to the external stream.

Experiments indicate that the balanced arc in a supersonic flow simulates an impervious cylinder of uniform cross-section inclined to the flow at an angle near the Mach angle and that an axial flow along the arc exists. The model, applicable at high values of the Lorentz convection parameter, is comprised of an inner core of nearly constant properties, and a boundary layer; circulation within the core carries the heat to the edge of the boundary layer, which then transfers it through conduction to the external flow.

10. REFERENCES

1. (a) Bond, C. E., "Magnetic Confinement of an Electric Arc in Transverse Supersonic Flow," AIAA J., 3, 142 (1963).
(b) Bond, C. E., "The Magnetic Stabilization of an Electric Arc in Supersonic Flow," Ph.D. dissertation, The University of Michigan (1964), also ARL 65-195, October, 1965.
(c) Bond, C. E., "Slanting of a Magnetically Stabilized Electric Arc in Transverse Supersonic Flow," Phys. Fluids, 9, 705 (1965).
2. Progress Report, February 28, 1965, Contract AF 33(657)-8819 and Final Report, June 1, 1965, Monitored by Thermomechanics Branch, Aerospace Research Laboratories, Wright-Patterson Air Force Base, Ohio.
3. (a) Roman, W. C., "Investigation of Electric Arc Interaction with Aerodynamic and Magnetic Fields," Ph.D. dissertation, Ohio State University (1965).
(b) Roman, W. C., and Myers, T. W., "Investigation of Electric Arc Interaction with Aerodynamic and Magnetic Fields," ARL 66-0191, Aerospace Research Laboratories, 1966.
4. Fischer, E., and Uhlenbusch, J., "D.C. Arcs in Transverse Force Fields," Seventh Symposium on Phenomena in Ionized Gases, 1965.
5. Jakob, M., Heat Transfer (John Wiley and Sons, Inc., New York, 1949), Vol. 1, p. 560.
6. John, R., Bade, W., and Liebermann, R. W., "Theoretical and Experimental Investigation of Arc Plasma-Generation Technology, Part II, Vol. 2, ASD-TDR-62-729, September, 1963.
7. Ragent, B., and Nobel, C. E., "High-Temperature Transport Coefficients of Selected Gases," ARL 62-328, April, 1962.
8. Mair, W. A., and Beavan, J. A., Ch. 12, Modern Developments in Fluid Dynamic—High Speed Flow, L. Howarth, Ed., p. 685, Oxford University Press, 1953.
9. Hoerner, S. F., Fluid-Dynamic Drag, 2nd Edition, published by author, 1965.

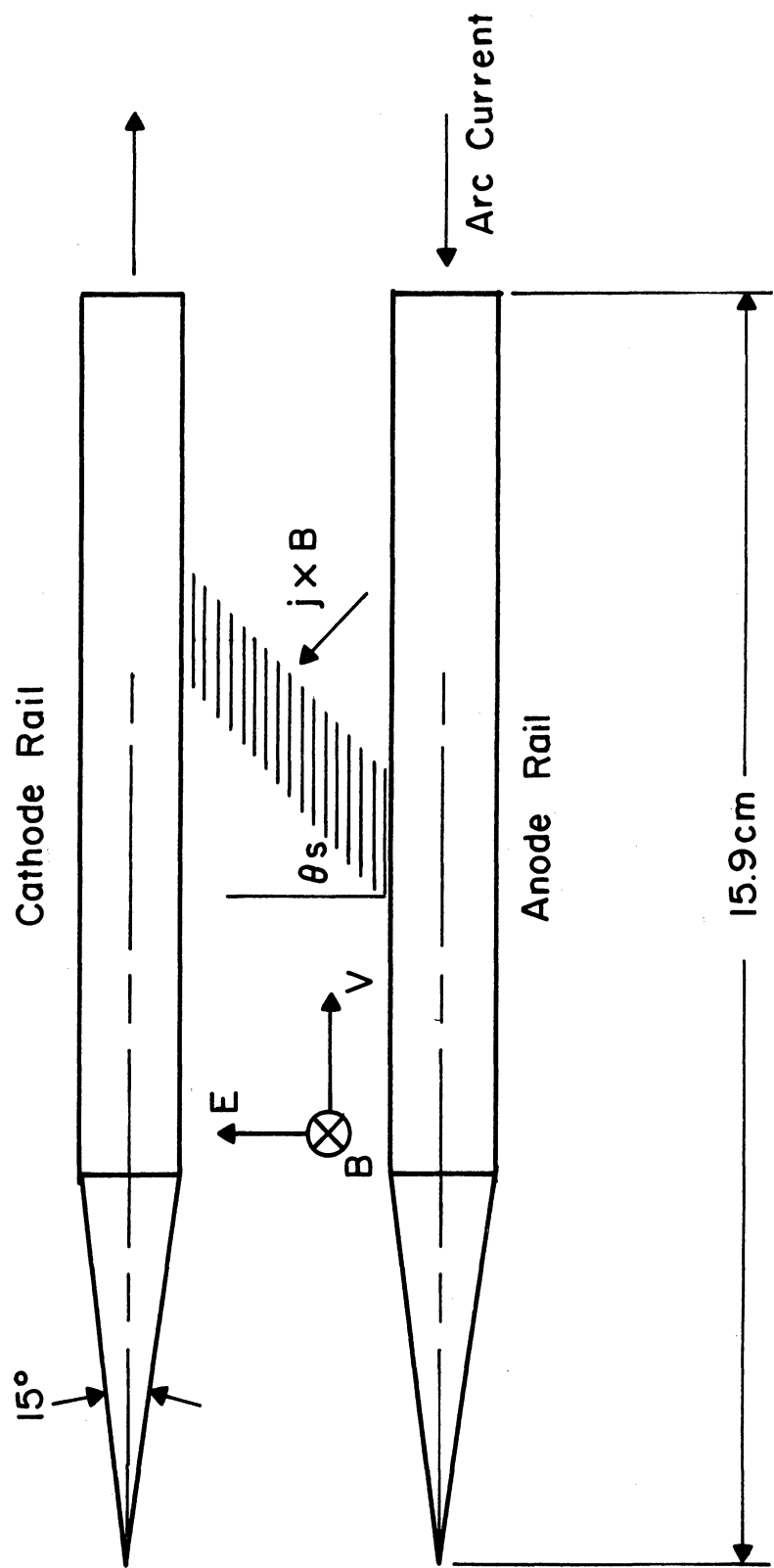


Fig. 1. Relative orientation of the velocity, magnetic, and electric fields.



Fig. 2. Polaroid photograph of arc reflection in side-wall of tunnel. $M_{\infty} = 2.5$, $P_t = 12.9$ in. Hg, $I = 425$ amp, gap = 1.1 in.

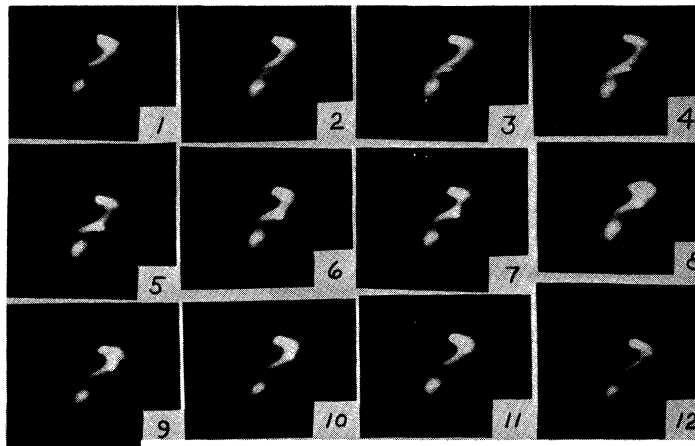


Fig. 3. Film sequence showing particle moving from anode (bottom) to cathode. $M_{\infty} = 2.5$, film speed about 3000 exposures per second.



1



2



3



5



4

Fig. 4. Film sequence showing two views of particle moving from anode (bottom) to cathode in the column wake. $M_{\infty} = 2.5$, film speed about 4700 exposures per second.

6

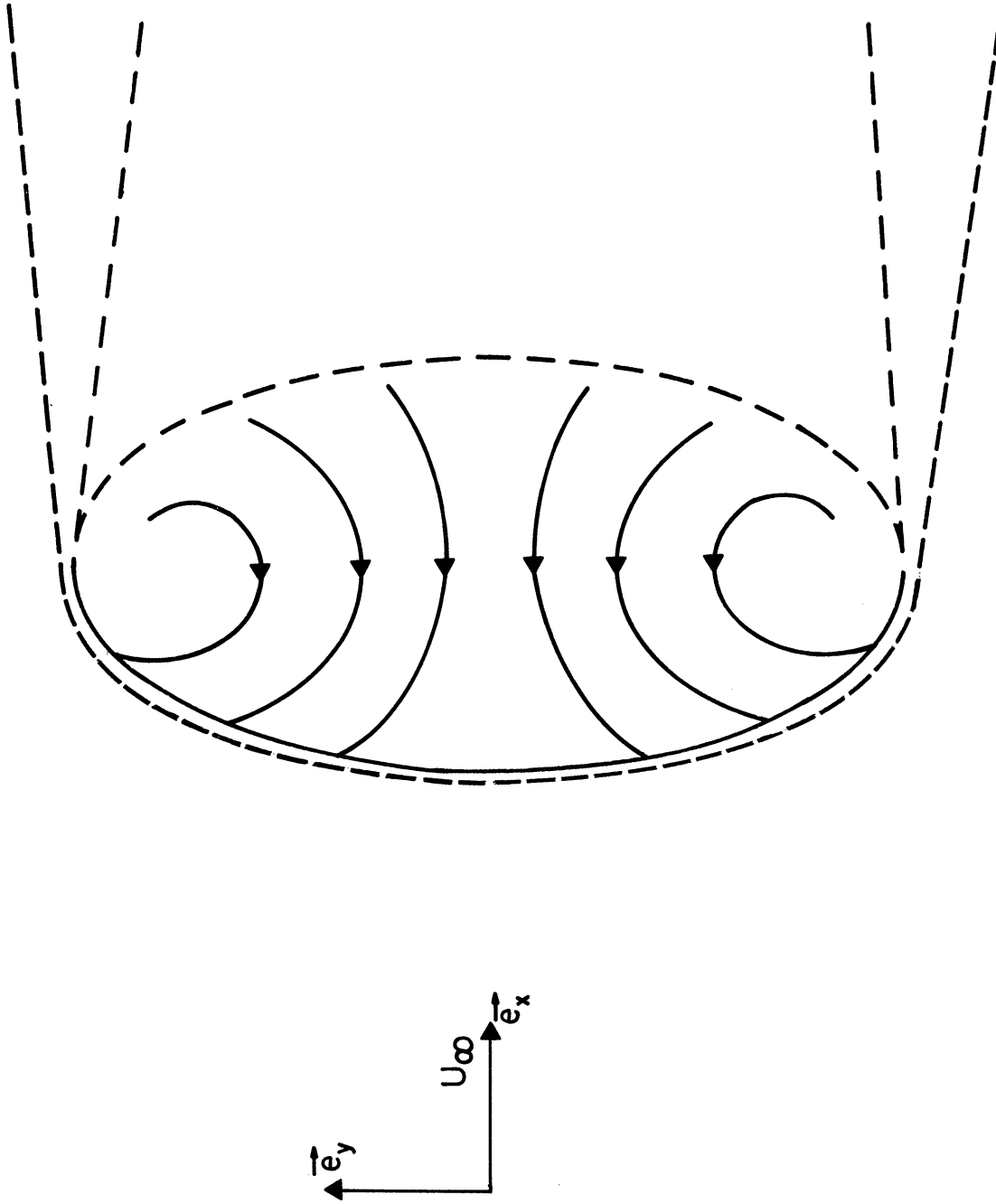


Fig. 5. Qualitative model of balanced arc.

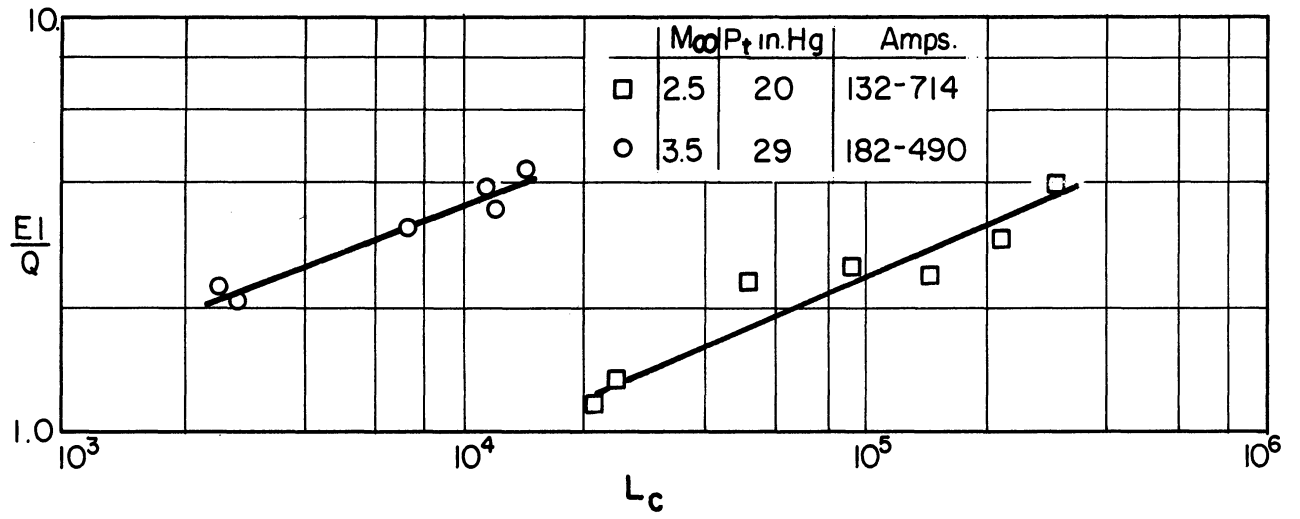


Fig. 6. Heat transfer from arc relative to that from solid cylinder versus Lorentz convection parameter.

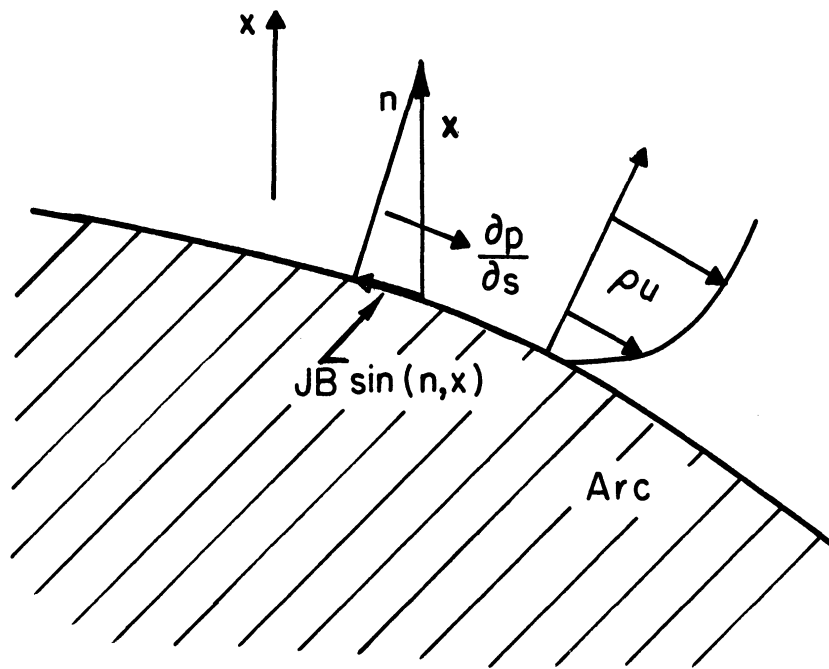


Fig. 7. Boundary layer formation.

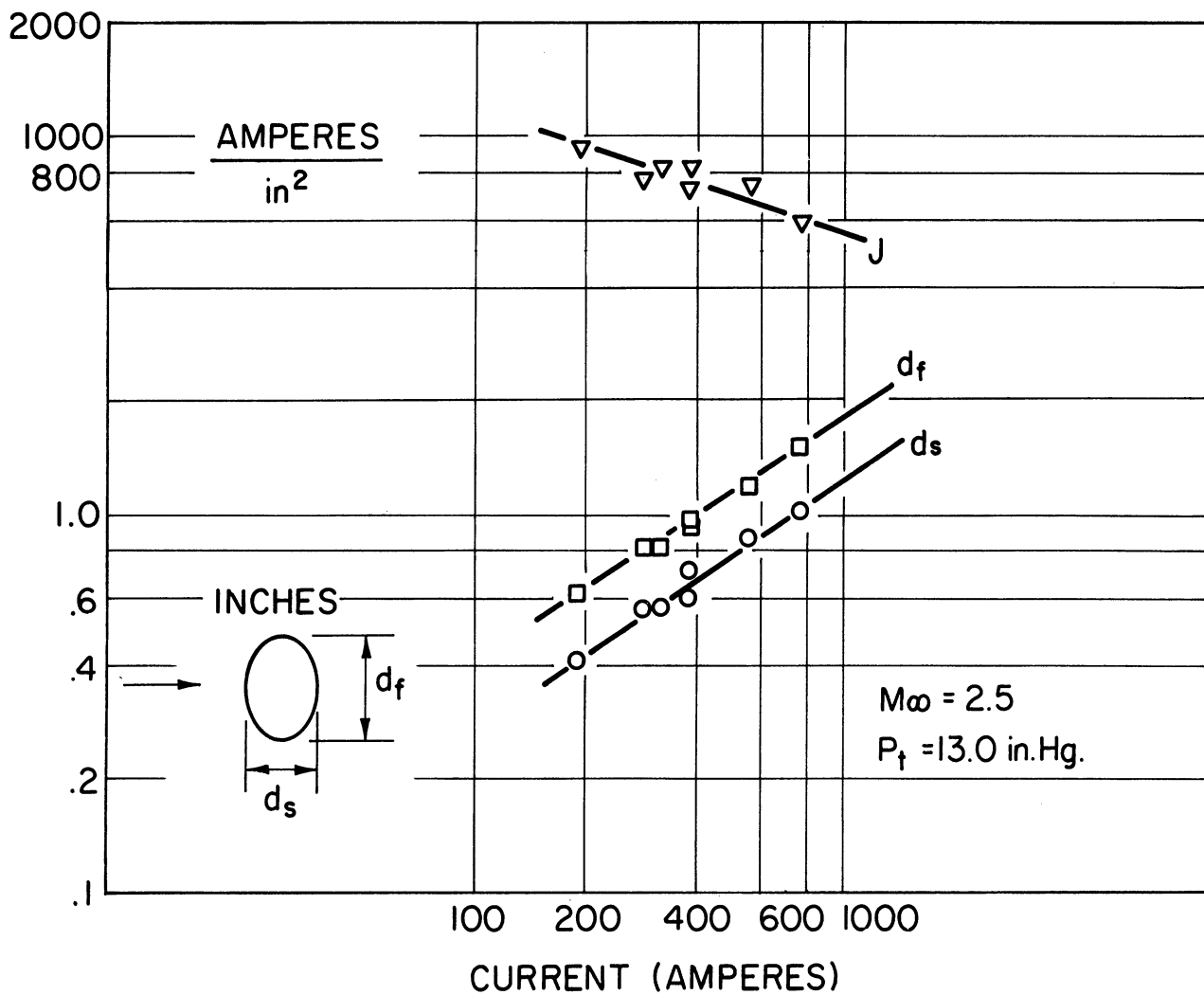


Fig. 8. Current density and arc dimensions for $M_\infty = 2.5$.

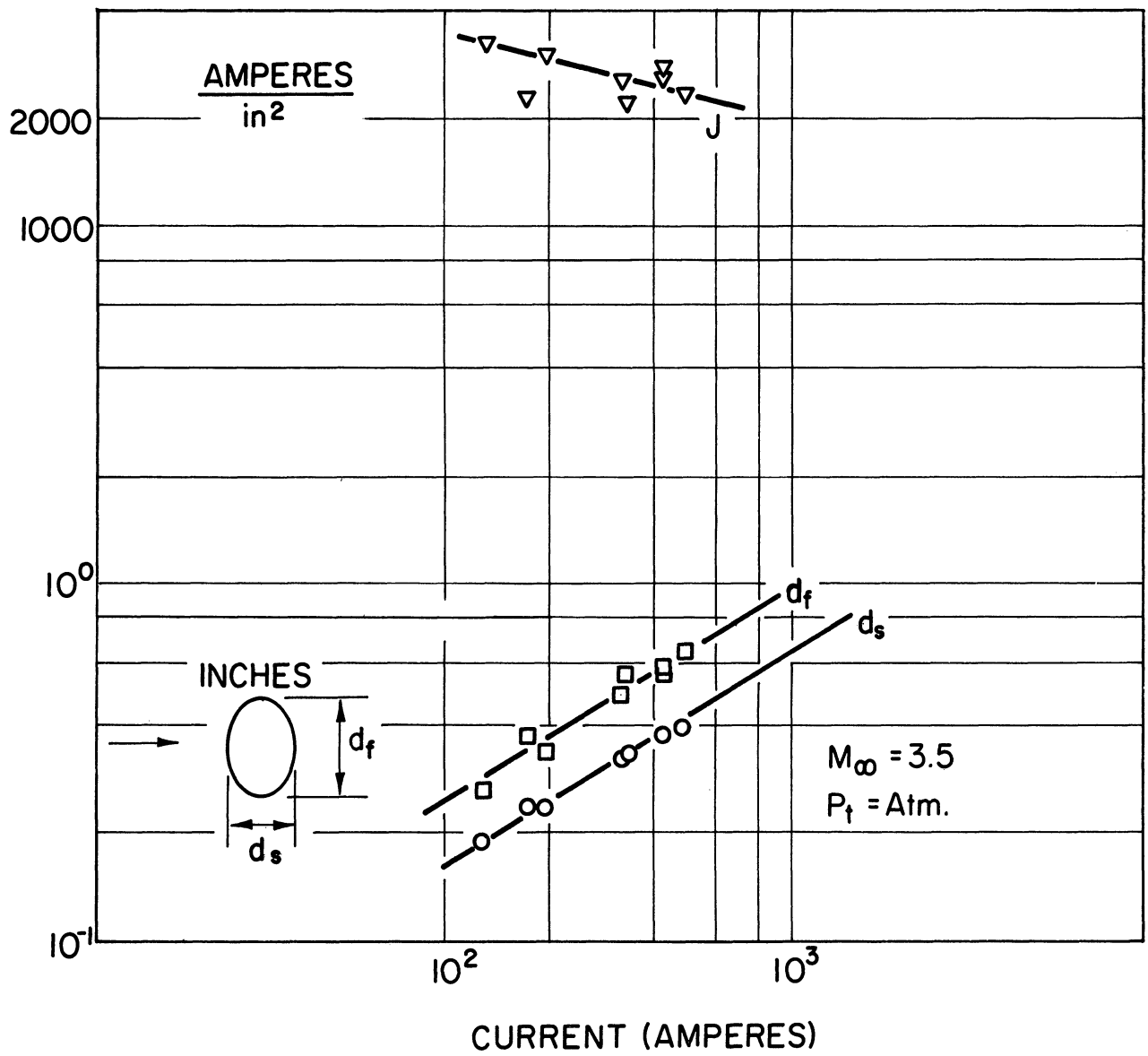


Fig. 9. Current density and arc dimensions for $M_\infty = 3.5$.

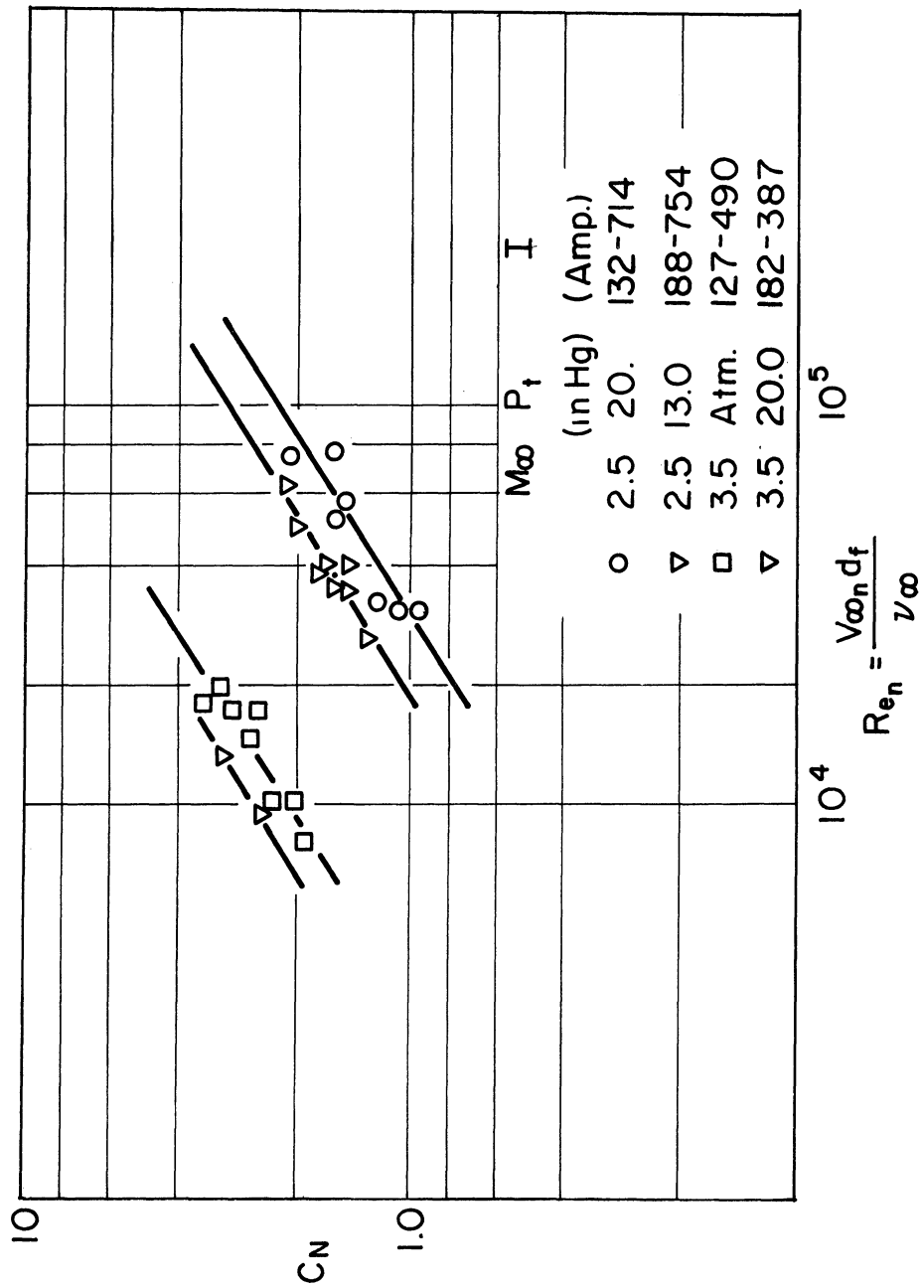


Fig. 10. Normal force coefficient referred to the normal velocity component versus the normal Reynolds number based upon free stream properties.

